Fe- and Mn-Enrichment in Middle Ordovician Hematitic Argillites Preceding Black Shale and Flysch Deposition: The Shoal Arm Formation, North-Central Newfoundland[1]

Volker Brüchert,[2] John W. Delano, and William S. F. Kidd
Department of Geological Sciences, State University of New York at Albany, Albany, NY 12222

ABSTRACT

The Middle Ordovician Shoal Arm Formation in the central volcanic belt of north-central Newfoundland consists of hematitic argillites overlain by grey cherts, then black shales directly underneath a Late Ordovician/Early Silurian flysch sequence. Using principal component analysis, geochemically definable components within related lithologic groups are: (1) biogenic, (2) mixed detrital, (3) hydrothermal, and (4) Mn,Ca-carbonate. Close sampling of the whole 350-m thick sequence provides reconstruction of variations among the sediment components through time. At the base of the hematitic section, a sharp increase in the hydrothermal component (enrichment in Mn, Fe, Ni, Pb, and Zn) decreases stratigraphically upward and disappears in the upper red Shoal Arm Formation. The Mn,Ca-carbonate component also decreases upward but persists into the grey cherts, indicating an additional source of Mn. The clastic component is largely mixed mafic/pelagic clay-like detritus with a strong pulse of Zr-, Nb-, and Y-rich detritus in the top of the hematitic unit. This latter component was derived from lateral equivalents of the alkaline/subalkaline Lawrence Head volcanics. The red hematitic argillites are not overall strongly Fe-enriched but represent the product of oxic bottom conditions under slower sedimentation rates than those of the earlier underlying sediments of the Wild Bight Group island-arc-derived volcaniclastics. The grey cherts mark a transitional stage between the hematitic sediments (oxic) and the black shales (anoxic). The change to increasingly O_2-deficient conditions is explained by either (*a*) an increase in the biological productivity in the overlying water column and basinwide synchronous development of anoxic porewaters (or seawater) by increased C_{org}-oxidation or (*b*) the diachronous subsidence of the basin floor into a deep-water anoxic layer as a result of the loading of the floor by an approaching accretionary thrust stack. In the second hypothesis, which we prefer, the anoxic water layer would permit significant lateral transport of recycled dissolved Mn^{2+} subsequently precipitated in more oxygenated parts of the basin. It would also explain the significant Mn-enrichment in the upper red Shoal Arm Formation and the grey cherts.

Introduction

Certain Paleozoic deep-marine sediments of the northern Appalachians show a distinctive sequence of sedimentary units progressing upward from Fe- and Mn-enriched, hematitic argillites to grey cherts, then black shales and finally flysch sediments. These sediments accumulated prior to and during the collision of an island arc and/or microcontinent with the North American continent by the Middle Ordovician (Nelson 1979; Dewey et al. 1983; Rowley and Kidd 1981). While widespread Mn and Fe enrichment in modern pelagic sediments is generally interpreted to result from the deposition of hydrothermal material released into the seawater at mid-ocean ridges (e.g., Glasby 1991; Dymond 1981; Heath and Dymond 1981; Stoffers et al. 1985), in these Ordovician cases an obvious metal source is missing, and sources other than hydrothermal enrichment have to be considered. Stratiform Mn-enrichment in sediments preceding or associated with carbon-rich shales has also been observed in some deep-marine Jurassic and mid-Cretaceous sediments (Pratt et al. 1991; Jenkyns 1980; Jenkyns et al. 1991; Scholle and Arthur 1980; Pomerol 1983). The Mn-enrichment in these sediments apparently took place during, immediately preceding, or shortly after an oceanic anoxic event (Pratt et al. 1991; Jenkyns

[1] Manuscript received July 6, 1993; accepted November 6, 1993.

[2] Current address: Department of Geological Sciences, Indiana University, Bloomington IN 47405.

[The Journal of Geology, 1994, volume 102, p. 197–214] 0022-1376/94/10202-009$1.00

1980; Jenkyns et al. 1991; Scholle and Arthur 1980; Pomerol 1983; Schlanger and Jenkyns 1976). Reduced, dissolved Mn was transported in an expanded O_2-minimum zone and subsequently precipitated and deposited on the continental margin under more oxidizing conditions (Jenkyns et al. 1991; Force and Cannon 1988; Frakes and Bolton 1984). The widespread occurrence of Middle Ordovician graptolitic black shales in the northern Appalachians and Europe (Nelson 1979; Kusky 1985; Rast and Stringer 1980; Rowley et al. 1979; McKerrow 1979; Hay and Cisne 1988; Leggett 1980; Williams and Rickards 1984) has also been related to O_2-depletion of seawater (Leggett 1980; Williams and Rickards 1984), suggesting a similar relationship between dissolved Mn-transport and seawater oxygen depletion as in the early Jurassic and the mid-Cretaceous.

The Shoal Arm Formation in north-central Newfoundland (Nelson 1979) is an example of the distinctive stratigraphic sequence identified above, and it has excellent exposure, well-documented stratigraphy, and a low degree of metamorphism. There is a good understanding of its tectonic history. This work aimed: (a) to establish a detailed, geochemical stratigraphic sequence ranging from the underlying clastics to the greywackes above; (b) to discriminate the various sediment components that contributed material to the Shoal Arm Formation to identify the component(s) responsible for the Mn- and Fe-enrichment; (c) to create a model that explains the geochemical variation in agreement with the general tectonic evolution of this part of the Taconic Orogen; (d) to compare the geochemistry of the Shoal Arm Formation with the geochemistry of units in a similar stratigraphic sequence in the Middle Ordovician Taconic Allochthon of New York State to test the model's validity. We report here only the results of a detailed investigation of the geochemistry of the Shoal Arm Formation and their general geologic and paleooceanographic implications.

General Geology of the Shoal Arm Formation and Adjacent Units

The Wild Bight Group, the Shoal Arm Formation, and the Gull Island Formation are in the Exploits zone of the central volcanic belt of northern Newfoundland (Dewey et al. 1983) (figure 1). A general description of the stratigraphy and structure of the Exploits zone is given in Dewey et al. (1983). The investigated sequence lies in the western part of the Exploits zone (figure 1). The oldest exposed lithologies are >8 km of volcaniclastics and minor volcanics of the Wild Bight Group (Nelson 1979), of early Ordovician and possibly late Cambrian age at the base. The Wild Bight Group passes conformably into the Shoal Arm Formation, characterized by siliceous argillites. Nelson (1979) reported a thickness of about 500 m for the Shoal Arm Formation. From bottom to top this formation consists of three major lithologies: (1) dark-brownish red, bright-red and purple, hematitic and manganiferous, siliceous argillites with less abundant interbeds of green, siliceous, somewhat coarser-grained volcaniclastics, the two lithologies displaying an irregularly spaced layering throughout the Shoal Arm Formation; (2) grey cherts with black laminae and characteristic black burrow fillings; (3) black, pyritiferous slates. The youngest rocks in this area are Late Ordovician to Early Silurian quartzofeldspathic turbidite sandstones and slates (flysch) about 1.3 km thick, the Gull Island Formation. Similar stratigraphic sequences can be seen to the east in the Point Leamington area (Kusky 1985), on the Fortune Harbour Peninsula (Helwig 1967), and on New World Island (Helwig 1967).

Stratigraphic Order of Samples

Three stratigraphic sections of the Shoal Arm Formation were examined in Badger Bay and named (according to their locations) as the Gull Island Section, the Shoal Arm Section, and the Beaver Bight Section, respectively (figure 2). The measured thicknesses of the three sections are different, related to tectonic thinning during folding, and/or thrust duplications. Due to the deformation, it is impossible to deduce with precision the original thickness of the Shoal Arm Formation. We cannot provide any detailed information on the time span that was involved in the deposition, because only the paleontological age of the black shales is known (Caradocian: *Nemagraptus gracilis zone*; Dean 1978). Two marker horizons aided in correlating the three sections. One is a single level with a characteristic color change from maroon to bright-red argillites—informally called the maroon-red color transition; the other is a characteristically buckled, pyrolusite-stained Mn,Ca-carbonate layer. Figure 2 shows the relative stratigraphic positions of the samples; a table of the final stratigraphic order of all samples with the recalculated positions of samples from the Shoal Arm Section and the Beaver Bight Section relative to the least-deformed Gull Island Section is available from *The Journal of Geology* Data Depository upon request. Samples were taken at intervals ranging from 10 cm to 7 m. 109 samples were

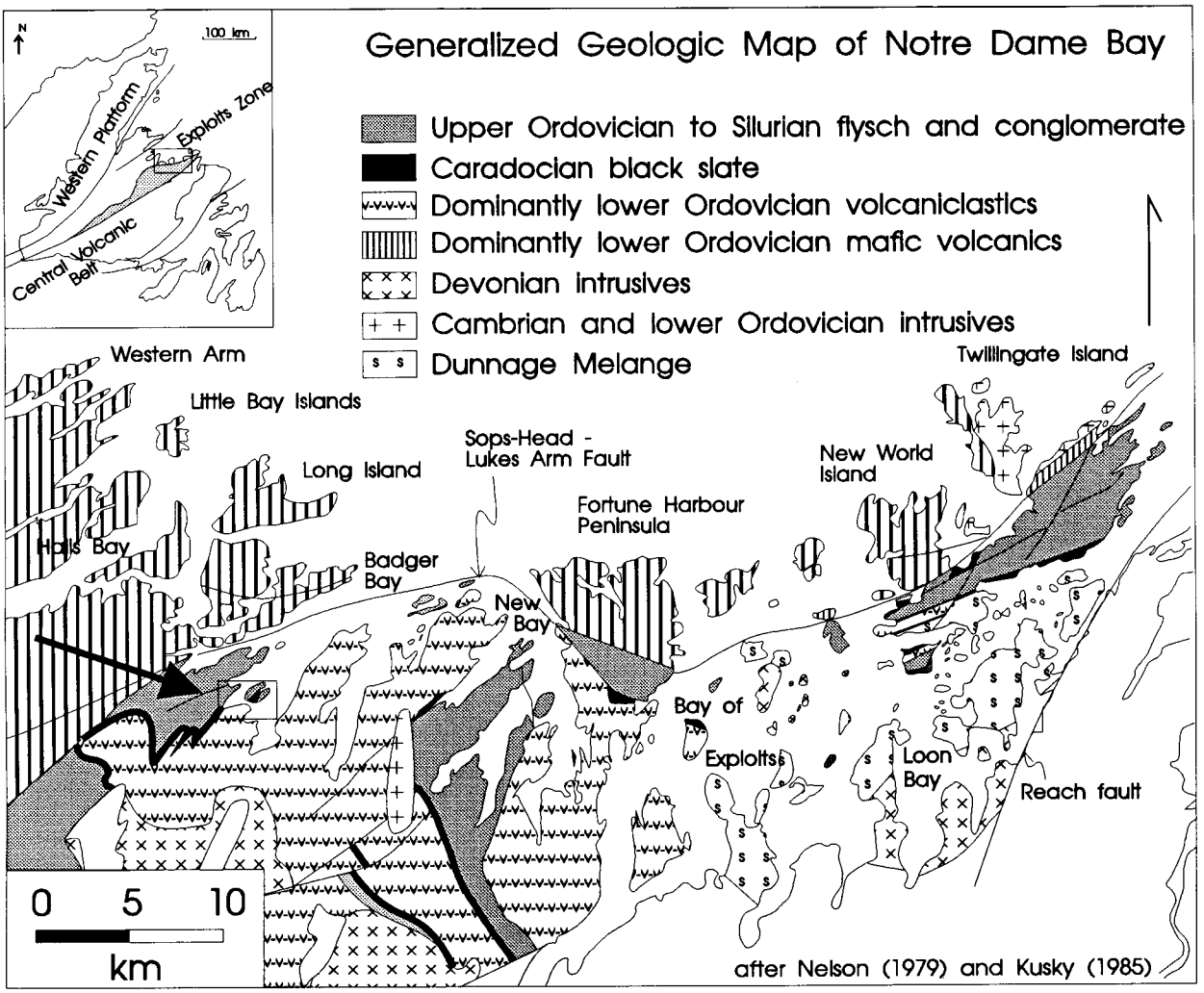

Figure 1. Generalized geologic map of the Notre Dame Bay. Arrow points to field area.

taken from the Badger Bay area, including those from the upper Wild Bight Group, the red, grey, and black Shoal Arm Formation as well as from the Gull Island Formation.

Sample Preparation and Analytical Procedures

Depending upon the grain-size, 500–1500 grams of rock sample were crushed, milled, and finally ground in a tungsten-carbide shatter box. About 25 grams of the homogenized powder per sample were selected and sent to Geochemical Laboratories, Department of Geological Sciences, McGill University, Montreal (analyst Dr. S. T. Ahmedali) for XRF-analysis of the following elements: Si, Ti, Al, Fe, Mn, Mg, Ca, Na, K, P, Ba, V, Cr, Ni, Co, Cu, Zn (on fused disks), Nb, Zr, Y, Sr, Rb, Pb, Th, and U (on pressed powder pellets). Analytical precision was tested with duplicate analyses of a department-internal standard of an Austin Glen shale from the Ordovician Taconic flysch of eastern New York State. The XRF analyses of all samples and the duplicate analyses of the Austin Glen Standard are available from *The Journal of Geology* Data Depository upon request. The analytical precision given by McGill was <0.3 wt % for the major elements and <8 ppm for the minor and trace elements. Detection limits were 0.01% for the major elements, 15 ppm for Cr_2O_3, 10 ppm for V, Ba, Co, Cu, and Zn, and 2 ppm for Nb, Zr, Y, Sr, Rb, Th, and U, except Pb (4 ppm).

Petrography and Fine-Scale Compositional Variation

The 25 thin-sections of red argillites, green, calcareous argillites, grey cherts, and greywackes have been examined under transmitted light using an electron microscope equipped with a backscattering electron detector. The mineral association of

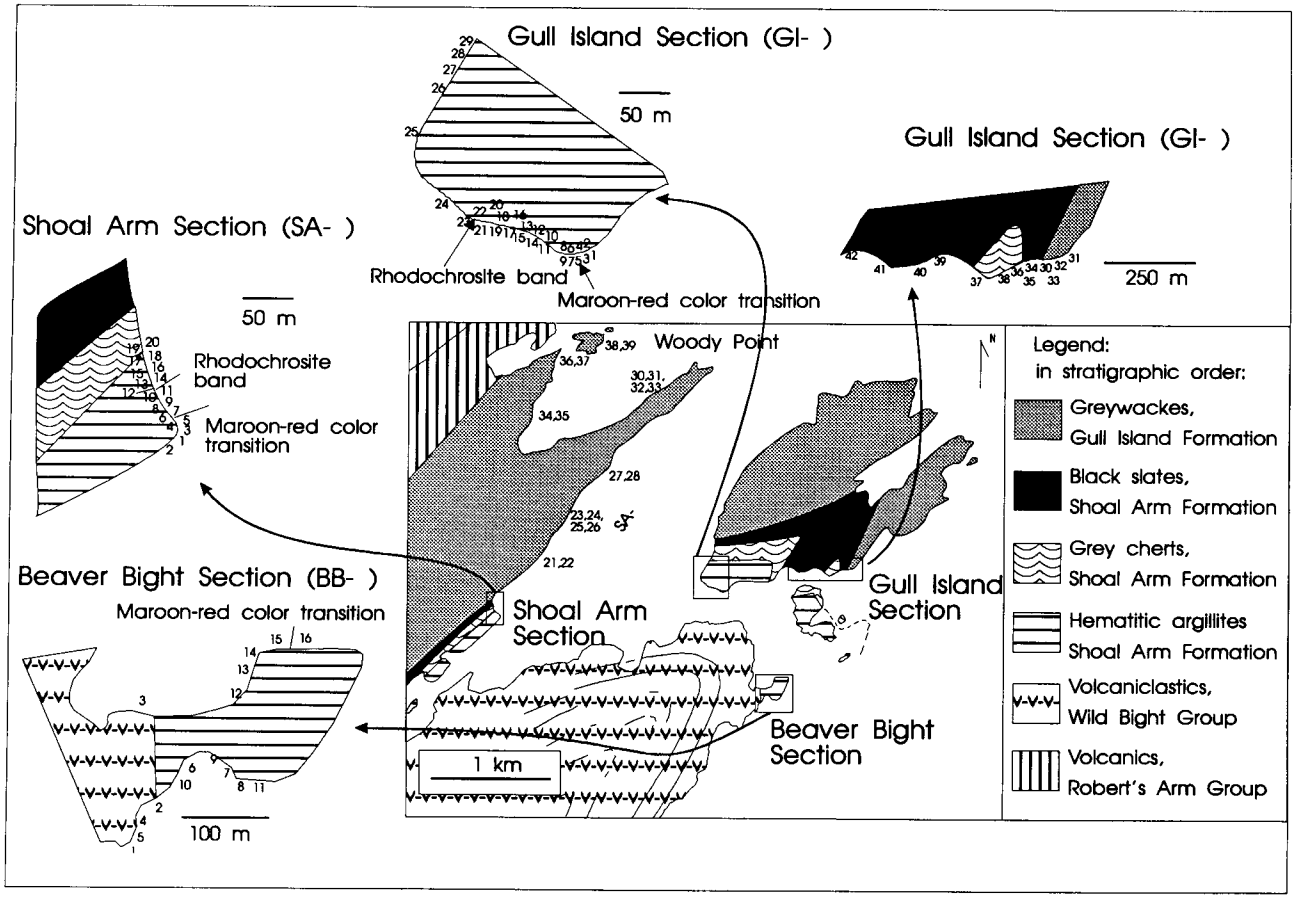

Figure 2. Geologic map of the field ara around Gull Island. Enlarged are the four measured sections. The numbers in each section indicate the locations of the samples.

all thin-sections is characteristic of the prehnite-pumpellyite/lower greenschist facies. Quartz, albite, muscovite, Mg-chlorite, finely dispersed hematite (in red argillites) and Mn,Ca-carbonate (in green argillites) are the major constituents of the argillites and cherts. Calcite, apatite, prehnite, titaniferous magnetite, and pyrite (only in green argillites) are accessory phases. The argillites are well sorted and have grain-sizes between 1 and 50 μm.

Quartz is the major constituent of red and green argillites and cherts. The mineral appears both in round to slightly elliptical bodies and finely dispersed in the matrix. The spherical bodies most likely represent recrystallized radiolarians. The fine-grained quartz in the matrix is presumably also partly biogenic and may be a product of recrystallization during diagenesis and low-grade metamorphism. Some of the fine-grained quartz may also be derived from a silicic volcanic source. The hematite has grain-sizes of <1 μm. Thin sections of the hematitic argillites show channels filled with coarser plagioclase-rich material and relatively large former radiolarians that cut into the underlying clay-rich material. These features support the field interpretation that the red argillites were deposited by silty turbidites. The silty intervals are less hematitic than the finer-grained tops. Hematite is more abundant in the clay-size intervals, supporting the interpretation that either the coarser grained, clastic component or the biogenic material have suppressed the hematite component. An independent Fe-source is thus necessary, possibly Fe-oxyhydroxides that were dehydrated during compaction and formed hematite.

Green argillites intercalating the hematitic argillites lack hematite but have increased Mn,Ca-carbonate and Fe-chlorite. These minerals are particularly abundant at the bottom of green argillitic interbeds; they are coarser-grained and replace the clastic matrix. Between 120 and 160 m these green argillites are consistently coarser-grained than the hematitic argillites. Across the color boundary from red to green argillites, carbonate significantly increases. Carbonate becomes the dominant phase in the pink Mn,Ca-carbonate band. Overlying this band, carbonate remains the dominant phase for at

least the next 3 cm, replacing the clastic matrix by approximately 75%. These characteristics suggest that the large phases are secondary and have been formed during diagenesis.

To assess the fine-scale compositional variation across these red-green color transitions, 99 large beam diameter (>30 μm) electron microprobe analyses were obtained from two thin-sections enclosing an interval of 4.7 cm across one of the color boundaries. Individual spots were oriented in rows parallel to bedding; 11 analyses on each of 5 rows in the red part and 4 rows in the green part. This procedure attempted to eliminate the compositional variation within a row caused by the different minerals. The mean and standard deviation were calculated for each row of 11 analyses (figure 3). These results indicated that the method can differentiate the different geochemical compositions of each row. For reference, the results were compared with whole-rock XRF-analyses of the red argillite (GI-2) underneath and the green argillite (GI-4) above the color transition.

MnO, CaO, SiO_2, BaO, and total Fe (expressed as FeO) all show distinct maxima at the bottom of the green argillite (figure 3). (The elements have been normalized to Al_2O_3 to avoid deceptive effects of SiO_2 dilution.) An excess of Mn is not balanced by the deficiency in the underlying red part—suggesting an external source of Mn. Mn may either have been derived from within the sediment by diagenetic mobilization (Okita 1992)—but from an array larger than the scale of observation—or it was directly precipitated from the seawater (Pedersen and Price 1982). Several lines of evidence support the first interpretation. (1) From standard optical petrography and outcrop observation, the green argillites exhibit sedimentary structures that support a turbiditic origin and suggest that the calcareous turbidites were derived from shallower parts of the basin. (2) Transmitted-light petrography and back-scattered electron imaging revealed that Mn,Ca-carbonate is clearly of secondary origin. (3) The maxima of the elements Si and Ba at the bottom of the green argillite may also represent a larger amount of biogenic material, possibly deposited as a biogenic turbidite. (4) Fe shows a characteristic saw-tooth pattern at the interface, suggesting a localized mass transfer of Fe by reduction, transport, and reprecipitation in the green, calcareous part. Fe reduction and mobilization requires a larger redoxpotential than Mn-reduction. The limited mobility of Fe seems to indicate that, under these diagenetic conditions, Fe did not migrate more than 3 cm, but Mn may have been mo-

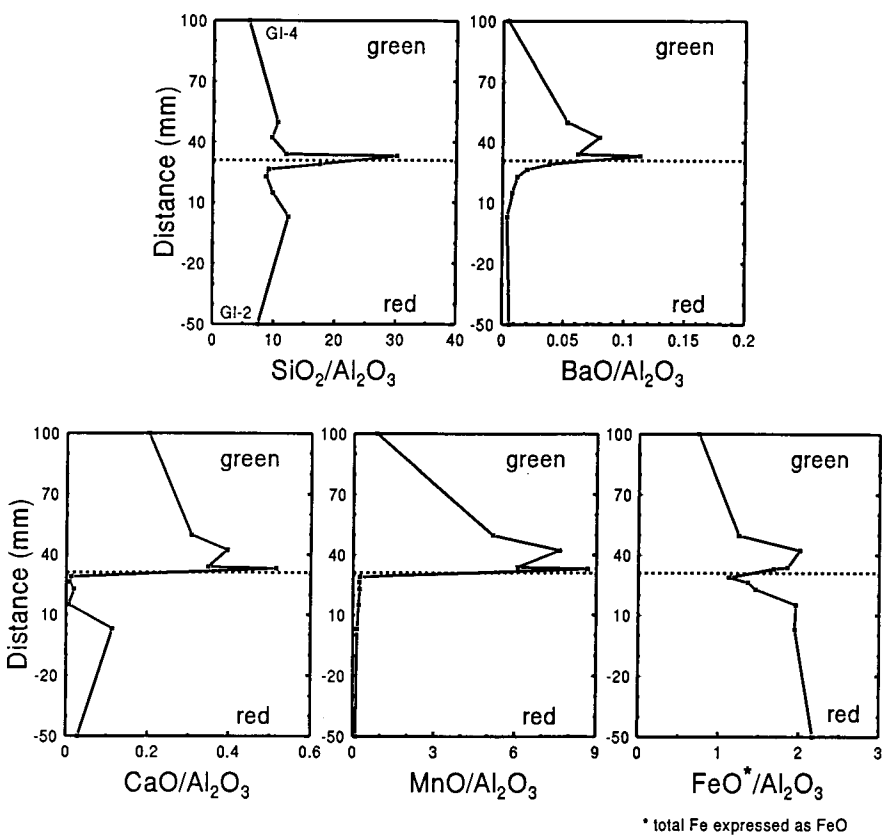

Figure 3. Mean and standard deviation of electron microprobe analyses of Mn, Fe, Si, Ca, and Ba across bed interface from red, hematitic to green, Mn,Ca-carbonate-bearing argillitic turbidite. The color transition marks a significant compositional boundary across which Mn and Fe were transported as reduced species and precipitated as carbonates after emplacement of a calcareous biogenic turbidite.

bile over a larger scale. Mn therefore seems also to be derived from the sediment and not from the seawater.

These observations support a model where upon emplacement of a calcareous, biogenic turbidite, Mn (and to a smaller extent, Fe) was reduced along a downward migrating oxidation front. The elements migrated upward into the turbidite and were reprecipitated as carbonates. Slight depletion of Ca in the top of the red part may suggest some dissolution of calcite. Increased HCO_3^- activities in the green part may have aided in the carbonate precipitation. An analogous situation has been reported by Thomson et al. (1986) where Mn-oxyhydroxides underlying a calcareous turbidite served as a source for Mn. Upon reduction, the element diffused upward into the turbidite, where it was fixed by absorption on calcite.

Discrimination of Principal Sediment Components

The petrographic variation within the whole stratigraphic sequence suggests important compositional differences between stratigraphic units. For this reason the data set was separated into lithologically related groups, in descending stratigraphic order: (1) greywackes and black slates; (2) grey mottled cherts; (3) Zr-rich argillites of the upper Shoal Arm Formation; (4) green argillites; (5) bright-red argillites; (6) Fe-enriched argillites; and (7) volcaniclastics of the upper Wild Bight Group. Table 1 lists representative geochemical analyses of these lithologic groups and compares them to three standard compositions. The different, sedimentary source components in the Shoal Arm Formation and the adjacent units were discriminated using correlation matrices. Greywackes and black slates were not used because the number of samples of each lithology was too small ($n = 6$) for a statistical analysis. Pearson correlation coefficients were calculated for all pairs of variables in each of the lithologically similar groups. Significance limits were determined by calculating the high and low confidence limits for a correlation coefficient. For positive correlation coefficients, the lower confidence limit had to be >0.5. In addition, the binary relationships were checked by binary graphs for outliers that could control the correlation coefficients. All elements in every data set were systematically plotted against Al_2O_3 and Fe_2O_3. Elements with high, positive correlation coefficients were combined into groups (figure 4). Well-correlated elements are connected with tie-lines. The different groups are spatially organized so that those with correlations just below the statistical cut-off are still located close to each other, to indicate their potential connection. Negative correlation coefficients were useful to confirm the different variances of groups of elements, expressed by spatial separation. Figure 4 is organized in ascending stratigraphic order, starting with the upper Wild Bight Group volcaniclastics in the bottom left corner, and ending with the grey cherts of the Shoal Arm Formation in the upper right corner. Dotted lines are drawn around groups suggestive of a characteristic component.

Results. Significant correlation coefficients ($r >$ 0.64) exist between Ti, Al, Cr, Rb, K, Ba, Na, Mg, Zn, Zr, Nb, and Y in the Shoal Arm Formation and the upper Wild Bight Group. Most of these elements are relatively immobile during diagenesis and are likely derived from detritus. There are particularly high correlation coefficients between Zr, Nb, and Y, which suggest that they have an individual source. The fact that relatively incompatible elements (e.g., Zr, Nb, and Y) are positively correlated with the compatible elements Cr, Mg, and V indicates a well-mixed clastic component. The elements may be derived from several, compositionally different, detrital source but have been blended subsequently into a single, undifferentiable component.

The Fe-rich, hematitic argillites and the bright-red argillites show associations of Fe, Co, and Ni, ± Pb and Zn. These elements can be discriminated from the other groups by low or negative correlation coefficients. The association may indicate a hydrothermal source, since these elements are typical constituents of hydrothermal fluids (e.g., Bischoff and Rosenbauer 1983; Seyfried and Janecky (1985) released into seawater at hydrothermal vents. Hydrothermally derived Fe in seawater is largely in particulate form as Fe-oxyhydroxides (Hudson et al. 1986). Fe-oxyhydroxide particles are capable of adsorbing trace elements (e.g., Co, Ni, or Pb) onto their surfaces (Förstner 1982*a*). The element association in this group thus may reflect the primary adsorption of the trace metals Co, Ni, and Pb onto possibly hydrothermally derived Fe-oxyhydroxides that were suspended in seawater. During diagenesis and metamorphism, the oxyhydroxides were dehydrated to form finely disseminated hematite. The hydrothermal component is not detectable in the upper Wild Bight Group. Discrimination of this component in the green, calcareous argillitic interbeds of the red Shoal Arm Formation is problematic because (a) Ni is apparently

Table 1. Representative Analyses of Samples from the Wild Bight Group, the Shoal Arm Formation, and the Gull Island Formation

Lithology	(a)	(b)	(c)	(d)	(e)	(f)	(g)	(h)			
Sample	GI-32	GI-41	GI-38	SA-16	GI-22	GI-2	GI-4	BB-13	(i)	(j)	(k)
SiO_2	59.42	88.77	92.52	80.31	82.12	64.87	58.88	79.31	62.80	56.70	55.34
TiO_2	.81	.21	.16	.16	.23	.49	.60	.20	1.00	1.11	.84
Al_2O_3	17.33	4.93	2.44	9.50	5.24	8.64	10.29	10.23	18.90	11.80	17.84
Fe_2O_3	8.03	.56	1.13	3.25	6.59	18.78	7.60	2.39	7.22	8.50	8.23
MnO	.07	.01	.15	.59	.96	.96	8.57	.44	.11	.07	.67
MgO	3.29	.31	.39	1.24	1.98	1.52	1.83	.64	2.20	2.80	.93
CaO	.46	.01	.57	.02	.13	.29	2.09	.38	1.30	. . .	3.42
Na_2O	2.58	.29	.37	4.01	1.12	1.05	1.80	5.04	1.20	1.39	1.53
K_2O	2.86	1.23	.67	.19	.33	1.63	1.43	.25	3.70	3.17	3.26
P_2O_5	.12	.01	.03	.03	.07	.21	.08	.04	.16	.18	.14
V (ppm)	155	117	16	22	10	72	66	29	150	460	120
Cr_2O_3 (ppm)	260	141	17	67	51	122	127	44	110	263	131
Ni (ppm)	108	10	10	10	31	70	55	10	55	186	225
Ba (ppm)	1278	906	1137	476	139	538	438	170	650	737	2567
Co (ppm)	38	10	10	10	78	160	98	10	. . .	59	74
Cu (ppm)	82	86	62	71	52	79	38	93	. . .	150	250
Zn (ppm)	101	10	10	67	78	48	67	55	. . .	320	165
LOI	4.82	3.56	1.34	1.27	1.51	1.88	7.81	1.22	6.00	. . .	. . .
Total	99.84	99.85	100.02	100.58	100.16	100.33	101.01	100.15	99.90	. . .	. . .
Nb (ppm)	11	4	9	38	9	11	14	18	19	. . .	14
Zr (ppm)	113	35	27	221	54	78	109	137	210	170	150
Y (ppm)	25	5	7	75	22	36	28	43	27	33	9
Sr (ppm)	51	9	56	75	21	20	34	37	200	. . .	18
Rb (ppm)	92	45	25	6	13	60	51	6	160	. . .	110
Pb (ppm)	21	5	5	7	11	35	4	4	20	. . .	80
Th (ppm)	11	7	5	11	6	6	7	13	15	. . .	5
U (ppm)	5	5	5	3	5	3	3	3	3	. . .	1

Note. Representative analyses of (a) greywacke of the Gull Island Formation; (b) black slate of the Gull Island Formation; (c) grey chert of the Shoal Arm Formation; (d) Zr-rich, green argillite of the Shoal Arm Formation; (e) hematitic argillite of the Shoal Arm Formation; (f) Fe-rich, hematitic argillites of the Shoal Arm Formation; (g) Mn-rich, calcareous argillite of the Shoal Arm Formation; (h) fine-grained volcaniclastic of the upper Wild Bight Group; (i) Post Archean Average Australian Shale (Taylor and McLennan 1985); (j) average of 28 Cretaceous shale analyses DSDP site 530 (on a carbonate-free basis) (Dean et al. 1984); (k) Average modern, Pacific, pelagic clay (Chester and Aston 1976).

partitioned between a clastic and a hydrothermal component, thus lowering the correlation coefficient and (b) diagenetic redistribution of elements was apparently more active than in the red argillites.

A correlation of Mn, Ca, Sr, and LOI (loss on ignition) ($r > 0.78$) can be identified in green argillites of the red Shoal Arm formation. Hematite-bearing argillites, grey cherts, black slates, and greywackes do not show this association. Although Mn is associated with Fe in the hydrothermal component of modern palagic sediments (e.g., Leinen 1987; Dymond 1981; McMurty 1981), in the Shoal Arm formation Mn does not correlate well with Fe or any of the associated trace elements in either red or green argillites. The correlation of Ca with Mn, Sr, and the LOI suggests the presence of Mn-carbonate. These findings agree well with the petrographic results and the microprobe work indicating that Mn mobilization and precipitation of Mn,Ca-carbonate took place at the color transition from red to green argillites.

In the Shoal Arm Formation and the upper Wild Bight Group, Si shows consistent negative correlation to all elements except Ba. Since Si does not correlate with immobile elements associated with a clastic component, most of the Si represents biogenic Si derived from radiolarians. This interpretation also agrees with the petrographic evidence. Ba and Si correlate in modern siliceous plankton (Martin and Knauer 1973), in diatomaceous sediments from areas of upwelling (Brongersma-Sanders 1983), and in modern deep-marine siliceous sediments (Calvert 1974), which also supports the interpretation of biogenic Si. Some of the Si may nonetheless also be of clastic origin, the negative correlation coefficients resulting from thorough sorting of the clastic fraction.

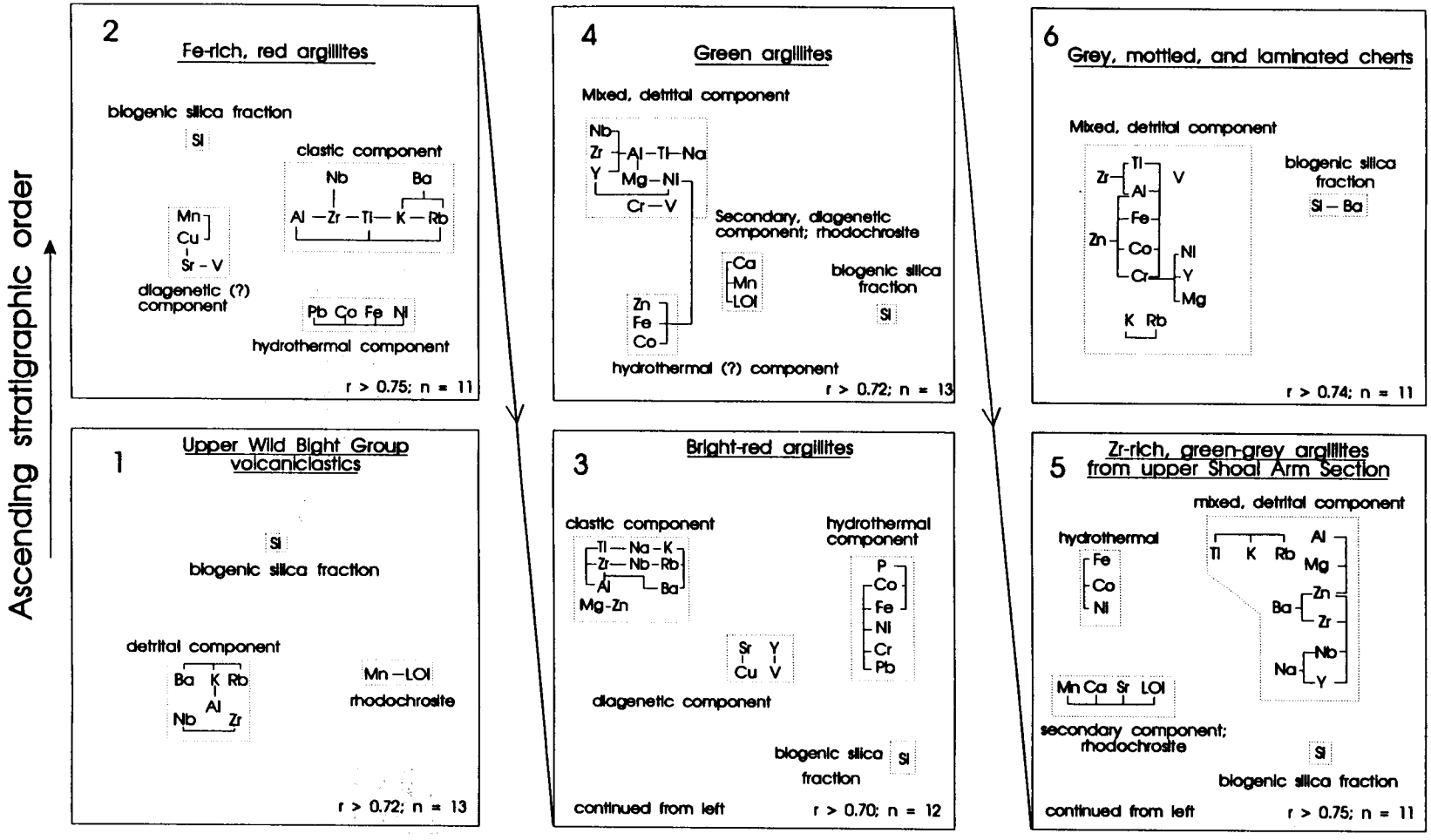

Figure 4. Illustration of the different, discriminated sediment components in the Wild Bight Group volcaniclastics (1), the Fe-rich argillites (2), the bright-red argillites (3), the green argillites (4), the Zr-rich, green-grey argillites of the upper Shoal Arm Section (5), and the gray, mottled, and laminated cherts of the grey Shoal Arm Formation (6) based on the analysis of element correlation coefficients. The lithologic groups are organized in ascending stratigraphic order starting from the lower left to the upper right. Although some of the Si is likely derived from the clastic fraction, only the biogenic fraction is reported, because no significant correlation coefficients exist to the elements representing the clastic fraction.

Stratigraphic Variation of the Compositional End-Members

Elements characteristic of each compositional end-member have been plotted against their stratigraphic position to gain qualitative insight into the stratigraphic variation of each source component (figures 5–8). To avoid deceptive effects of dilution by a third element (i.e., biogenic Si), elements were normalized to Al, because this element is generally considered to be immobile during diagenesis and its abundance may be moderately constant in lithologies with consistently small grain sizes (Argast and Donnelly 1987). This ratio has also been normalized to an average modern Pacific pelagic clay composition (Chester and Aston 1976) or the Post-Archean-Australian-Shale (PAAS)-composition (Taylor and McLennan 1985) to evaluate deviation from a standard composition. Ratios are interpreted in the following way: R = 1 means sample and reference composition are equal; R < 1 means that the sample is depleted in the normalized element relative to the standard; R > 1 means that the sample is enriched in the normalized element relative to the standard.

Detrital Source Variation. The interval 220–245 m shows a pronounced increase in Zr and a corresponding decrease in Cr and Ti (figure 5). Zr and Nb abundances in these argillites are as high as 351 ppm for Zr and 60 ppm for Nb. The clastic component is dominated by a Zr-, Nb-, and Y-rich component with low Ti and Cr. The increase in Zr cannot be explained by a grain-size increase or sorting, because the Zr-rich samples show no obvious difference in grain-size compared to the other samples, and no obvious zircon was detected in thin-sections using backscattered electron imaging and standard optical microscopy. Instead of detrital zircon, the clay component may have been the carrier of Zr in the Shoal Arm Formation argillites. The increase in the Zr/Al_2O_3 ratio is associated with similarly strong increases in the Y/Al_2O_3 and Nb/Al_2O_3 ratios. The Zr-Nb-Y-rich group is interpreted to reflect the original source-rock composition of a volcanic source, which became dominant in the upper part of the red Shoal Arm Formation. The source lithology of this component may have been alkaline basalts that can contain as much as 1000 ppm Zr, 126 ppm Nb, and 50 ppm Y (Basaltic Volcanism Study Project 1981). The Lawrence Head volcanics, characterized as sub-alkaline to alkaline basalts (Swinden et al., 1990; Jacobi and Wasowski 1985; DeLong unpubl. data) contain up to 526 ppm Zr, 85 ppm Nb, and 57 ppm Y (Swinden et al. 1990; DeLong unpubl. data). Thin sections of these samples also show no accessory zircons. No other analyzed volcanics in the Badger Bay–Seal Bay area or on the fortune Harbour Peninsula have comparably high abundances of these elements. It cannot be said whether this volcanic complex was active at the time of deposition or whether it was already inactive and being eroded by that time.

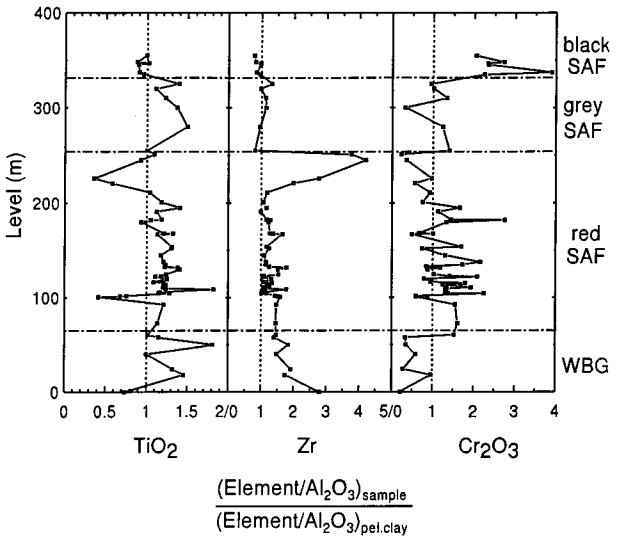

Figure 5. Stratigraphic variation of normalized detrial elements of different clastic sources in the upper Wild Bight Group (WBG) and the Shoal Arm Formation (SAF). Discriminated clastic sources are represented by Ti, Cr, and Zr. Vertical dotted lines mark equal composition to the modern Pacific pelagic clay standard (Chester and Aston 1976). The normalization to the standard is discussed in the text. Most significant is the Zr increase in the upper red Shoal Arm Formation, which may represent erosion of the Lawrence Head volcanics. The high Zr abundances correspond to high abundances of Nb and Y. The Cr-enrichment in the middle red SAF may represent enhanced contribution from mafic detritus.

In the 100–200 m interval Cr is slightly enriched relative to the modern Pacific pelagic clay, which may suggest the contribution of mafic volcanic detritus. The red argillites contain as much as 122 ppm Cr_2O_3. However, since related elements of potential mafic detrital origin (i.e., Mg and V) seem to be generally more mobile during diagenesis (Jarvis and Higgs 1987), this hypothesis is difficult to constrain. Ni could not be used since it is partitioned between the hydrothermal component and the mafic detrital component. The sharp increase in Cr in the black slates is a typical characteristic of black shales deposited under anoxic conditions, where elevated Cr abundances have been suggested to result from bioconcentration, biological sorption, and precipitation processes (e.g., Vine and Tourtelot 1979; Dean et al. 1984).

The alternative explanation that the Cr-enrichment signals the arrival of chromite-containing detritus, as seen in the overlying greywackes (Nelson and Casey 1979), is much less plausible because (a) Cr abundances in the greywackes are lower than in the black slates, and (b) ternary plots of detrital elements (i.e., Cr, Zr, Ti, Al, K) showed that the detrital component of the black shales is geochemically indistinguishable from the mixed detrital component in the Shoal Arm Formation.

The Hydrothermal Component. Pb, Fe, Co, and Ni are most strongly enriched at the 110 m level (figure 6). This interval is therefore interpreted to have the strongest hydrothermal influence. At this level, the hematitic argillites contain as much as 21.65 wt % total Fe (expressed as Fe_2O_3), 91 ppm Ni, 210 ppm Co, 51 ppm Pb, and 125 ppm Zn. Enrichment of these four elements continuously decreases upward. The Zr-, Nb-, and Y-rich argillites high in the red unit have the lowest abundances of these four elements in the red Shoal Arm Formation and therefore do not have a strong hydrothermal component. Elevated abundances of Pb and Ni in the grey Shoal Arm Formation are not associated with Fe and Co, which indicates a non-hydrothermal, possibly biogenic component for these two elements at this stratigraphic level. Mn may also be contributed from a hydrothermal component (e.g., Heath and Dymond 1977). The proximity of the Fe- and Mn-peaks around 110 and 140 m (figures 6 and 7) strongly suggests that, at this level, Mn is also of hydrothermal origin. Comparison of the trends of Fe and Cr (figures 5 and 6) indicates that the strongest Fe-enrichments do not coincide with the strongest Cr-enrichments. A more detailed examination of the corresponding trends by comparing each sample also showed that there is no consistent relationship between Fe and Cr, which makes it unlikely that the strong Fe-enrichment was caused by the contribution of mafic detritus.

Calcium Carbonate in the Shoal Arm Formation. Peak abundances of Ca in the red Shoal Arm Formation indicate a decreasing trend stratigraphically upward (figure 7). (Note: In this case the ratios have been normalized to the post-Archean-Australian-shale [PAAS] composition [Taylor and McLennan 1985], since no LOI-values are available for the average Pacific pelagic clay composition in Chester and Aston [1976]). Samples most strongly

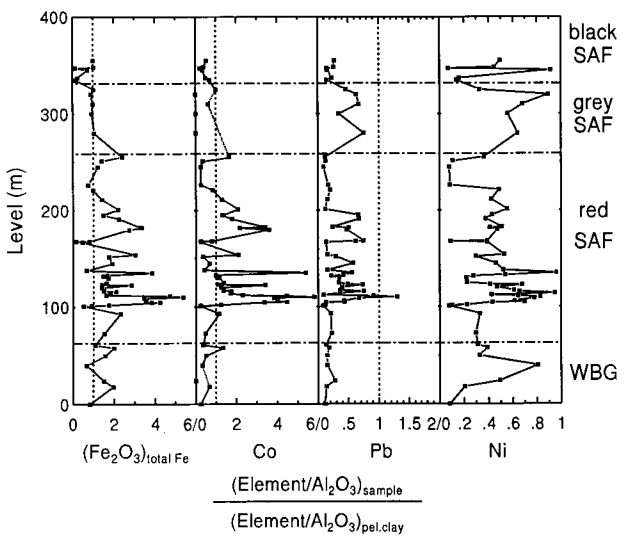

Figure 6. Stratigraphic trends of the "hydrothermal" elements Fe, Co, Pb, and Ni. The hydrothermal influence is strongest at the 110 m level and lowest in the interval of the Zr-rich argillites. The low normalized Ni/Al_2O_3 and Pb/Al_2O_3 ratios are explained by anomalously high abundances of these elements in the average pelagic clay composition. Fe, Co, and Pb are well correlated throughout the red Shoal Arm Formation, whereas Ni correlations only at around 110 m. The differing Ni-trend is interpreted by additional contribution from a mafic source and/or diagenetic redistribution.

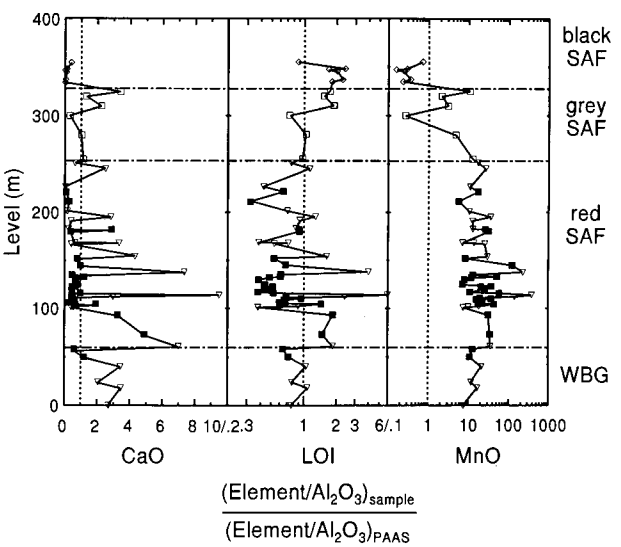

Figure 7. The stratigraphic variation of $CaCO_3$, represented by LOI (loss on ignition) and CaO, and MnO. Note the different scales on the x-axes. Filled squares represent red argillites, inverse triangles represent green argillites. Frequent Mn,Ca-carbonate is present only in those samples with elevated CaO and LOI. Since MnO levels are high throughout the Shoal Arm Formation, carbonate is suggested as the limiting parameter for Mn,Ca-carbonate formation. With the exception of one purple argillite, only intercalated green argillites show higher $CaCO_3$. These argillites represent calcareous turbidites.

enriched in Mn (i.e., 13.71 wt % MnO), contain substantial Mn,Ca-carbonate, and therefore exhibit corresponding peaks of LOI, CaO, and MnO. In contrast to CaO and LOI, MnO remains approximately constant in the red Shoal Arm Formation except for the two markedly enriched intervals at 110 and 140 m. Since both Fe and Mn are strongly enriched at this latter level (figures 6 and 7), Mn is also of hydrothermal origin. However, the consistent enrichment in Mn throughout the upper Wild Bight Group and the red and grey Shoal Arm Formation requires an additional source for Mn.

It appears that the amount of Mn,Ca-carbonate present depended on the availability of carbonate, since the Mn abundances are still relatively high in the upper stratigraphic levels of the red Shoal Arm Formation. Since pelagic calcareous organisms may have been insignificant in the Ordovician (Bruton 1984) and the green sediment beds show characteristics of calcareous turbidites, the calcium carbonate was probably transported as bioclastic turbidites from shallow-water environments. This source area may have been similar to the Cobbs Arm limestone on New World Island, which also underlies Caradocian black shales (Arnott et al. 1985). The decrease in CaO and LOI in the red and grey Shoal Formation may be explained by (1) gradual subsidence and/or erosion and eventual disappearance of the carbonate source; (2) ponding of the calcareous sediment in other parts of the basin; (3) subsidence of the basin below the CCD so that fewer calcareous, biogenic particles reached this depositional site.

Biogenic Si in the Grey Cherts. SiO_2 and BaO exhibit similar stratigraphic trends and show a pronounced increase in the grey cherts (figure 8). In these cherts, SiO_2 and BaO abundances are as high as 92.15% and 2754 ppm by weight, respectively. A correlation of Si with Ba in modern siliceous plankton is well documented (e.g., Martin and Knauer 1973; Calvert 1974) and suggests that the increase in these two elements in the grey unit reflects increased biological production in the near-surface seawater and an increase in the biogenic accumulation rate during deposition of the laminated and mottled grey cherts. Figure 8 shows that both the BaO/Al_2O_3 and SiO_2/Al_2O_3 ratios decrease again in the black slates, back to the level of the red Shoal Arm Formation. Although clearly more data would be needed, the BaO/Al_2O_3 ratio appears to decrease further upward to the uppermost sample of the sequence. Since this sample is a silty, black argillite (GI-32), and is probably a distal greywacke, during black slate deposition the biogenic component was likely diluted with clastic material. Alternatively, the increased production of radiolarians disappeared upon deposition of the black slates.

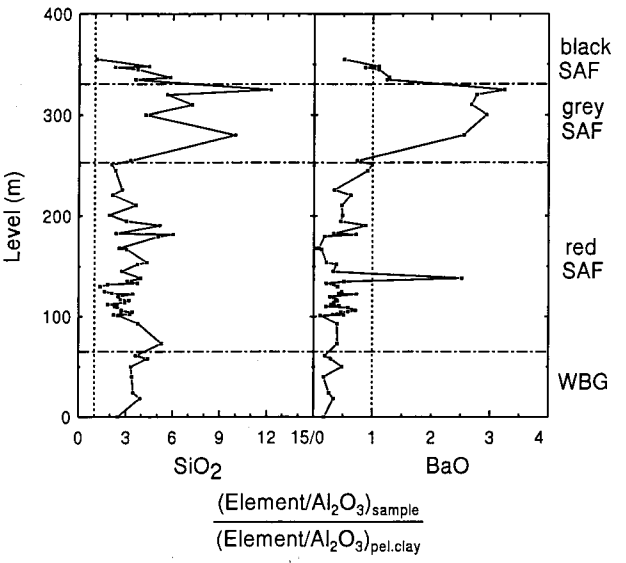

Figure 8. Normalized, stratigraphic trends of SiO_2 and BaO. The increased SiO_2 and BaO in the grey cherts may reflect increased biological productivity in the near-surface seawater. The low Ba ratios in the red Shoal Arm Formation compared to the Pacific pelagic clay are explained by anomalously high abundances of Ba in the average modern, Pacific, pelagic clay composition. The decrease of the Si and Ba in the black slates suggests either a decrease in the production of radiolarians during black shale deposition or enhanced deposition of detrital material and dilution of the biogenic component.

Models for the Depositional History of the Shoal Arm Formation

Central to the depositional history of the stratigraphic sequence is an interpretation of the change from oxic (red argillites) to anoxic (black slates) depositional conditions. The deoxygenation may reflect a change in the diagenetic environment, where the porewaters became increasingly anaerobic and diagenetic processes finally included bacterial suface reduction (Froelich et al. 1979) and the formation of diagenetic pyrite in the black shales (e.g., Berner 1984). Alternatively, the deoxygenation may reflect a transition from aerobic to dysaerobic to anaerobic (anoxic ?) conditions in the overlying water column. The low time resolution of this Middle Ordovician sequence poses an additional problem. It is not exactly known whether (a) the deposition of the red and grey unit ended simultaneously with the onset of deposition of the black shales in every part of the basin, or whether

(b) the deposition of the top parts of the red Shoal Arm Formation, and the grey and black Shoal Arm Formation was a time-transgressive, diachronous process that took place as a result of thrust-loading induced subsidence from the northwest (e.g., Nelson 1979, 1981; Arnott et al. 1985). Two contrasting models are consistent with the information available.

Figures 9 and 10 illustrate the evolution of the depositional basin, based on the work of various authors on the regional geology of the Exploits zone (i.e., Nelson 1979; Kusky 1985; Arnott et al. 1985; van Der Pluijm and van Staal 1988; Pickering et al. 1988; and Swinden et al. 1990). The Early Ordovician (Tremadocian-Arenigian-Llanvirnian) sedimentation in the basin is characterized by the deposition of mainly sandy, volcaniclastic material from an active volcanic arc (figures 9.I and 10.I). The volcaniclastics are represented by the Wild Bight Group and New Bay Formation. Since the proportion of volcanics to volcaniclastics decreases to the east and southeast (Helwig 1967; Arnott et al. 1985), the detrital source was probably to the west or nothwest. The transition from the sandy/silty volcaniclastics of the Wild Bight Group to the oxic argillites of the red Shoal Arm Formation suggests a decrease in volcanic arc activity and consequently a decrease in relief (figure 9.II and 10.II). Volcanic activity at this time is noted in the Lawrence Head volcanics. Based on the chemistry of these volcanics, which show an enriched (E-) MORB signature (Swinden et al. 1990; Jacobi and Wasowski 1985; Kidd et al. unpub. data), it is unlikely that the Lawrence Head volcanics were part of the arc complex. Kidd et al. (1977) related the Lawrence Head volcanics (and the Coaker Porphyry and gabbro intrusives in the Dunnage Mélange and in the New Bay Formation) to a subduction of an active spreading ridge into the Dunnage trench. Field observations show that the Lawrence Head volcanics were extruded in a submarine environment and suggest that they were active when the red shales of the Shoal Arm Formation were deposited elsewhere in the basin: (a) these volcanics are the only ones that directly underlie Middle Ordovician red shales equivalent in age to the red Shoal Arm Formation; (b) only a thin veneer of red shales is seen overlying the Lawrence Head volcanics; (c) maroon argillites comparable to the red Shaol Arm Formation occur in the lower part of the Lawrence Head volcanics. Based on these observations, it is suggested that hydrothermal activity during the Lawrence Head volcanic event is responsible for the enrichment of Fe, Mn, Ni, Co, Pb, and Zn in the lower red Shoal Arm Formation. This interpretation is supported by the association of blue chert and calcite interstices with sulfide minerals in pillow lavas of the Lawrence Head volcanics (Kusky 1985). Kusky (1985) suggests that these features resemble those found near submarine hydrothermal springs along ridge axes. Based on the available data, the Early Ordovician island arc (represented by volcanics of the Robert's Arm Group) is not considered to be the location of hydrothermal activity. Two red argillites of the Side Harbour Formation (part of the Wild Bight Group, (Nelson 1979) were not hydrothermally enriched, although these samples probably had the same general detrital source lithology as the argillites of the lower red Shoal Arm Formation.

Since the hydrothermal component fades in the upper part of the Shoal Arm Formation, Lawrence Head volcanism apparently ceased by the end of deposition of the red Shoal Arm Formation. However, the exact timing of this event is uncertain. Consequently, the Zr-, Nb-, and Y-rich components in the argillites of the upper red Shoal Arm Formation may be explained either by erosion of an active volcanic area, or by continued volcanic activity of equivalents of the Lawrence Head volcanics. In the beginning, these volcanics may have been restricted to deep water and thus contributed few clastics to the Shoal Arm Formation. With time, it may have been gradually built up to shallower/subaerial depths with its clastic contribution into the adjacent basin increasing in importance.

The tectonic evolution of the basin can subsequently be interpreted in two ways. The first proposes further subsidence of the basin and the development of quiet, pelagic conditions (figure 9.III). Since the late Llandeilo-Caradoc marks a time of high sea level (Leggett 1980), the adjacent island arc would have been relatively submerged and subject to minor erosion. Low clastic sedimentation rates would thus be expected. Several authors argue for a substantial global, eustatic sea-level rise in the Caradocian (e.g., Thickpenny and Leggett 1987; Leggett et al. 1981; McKerrow 1979). Leggett et al. (1981) relates the deposition of black shales in the Caradoc to global greenhouse effects—high sea level, higher marine temperatures, reduced oceanic circulation, stratified waters, and a high biological diversity.

In this case, the high Si and Ba abundances in the laminated and burrowed grey cherts of the grey Shoal Arm Formation may reflect nutrient-rich waters in upper mid-water levels that supported a flourishing, near-surface, siliceous phytoplankton community. This high biological productivity

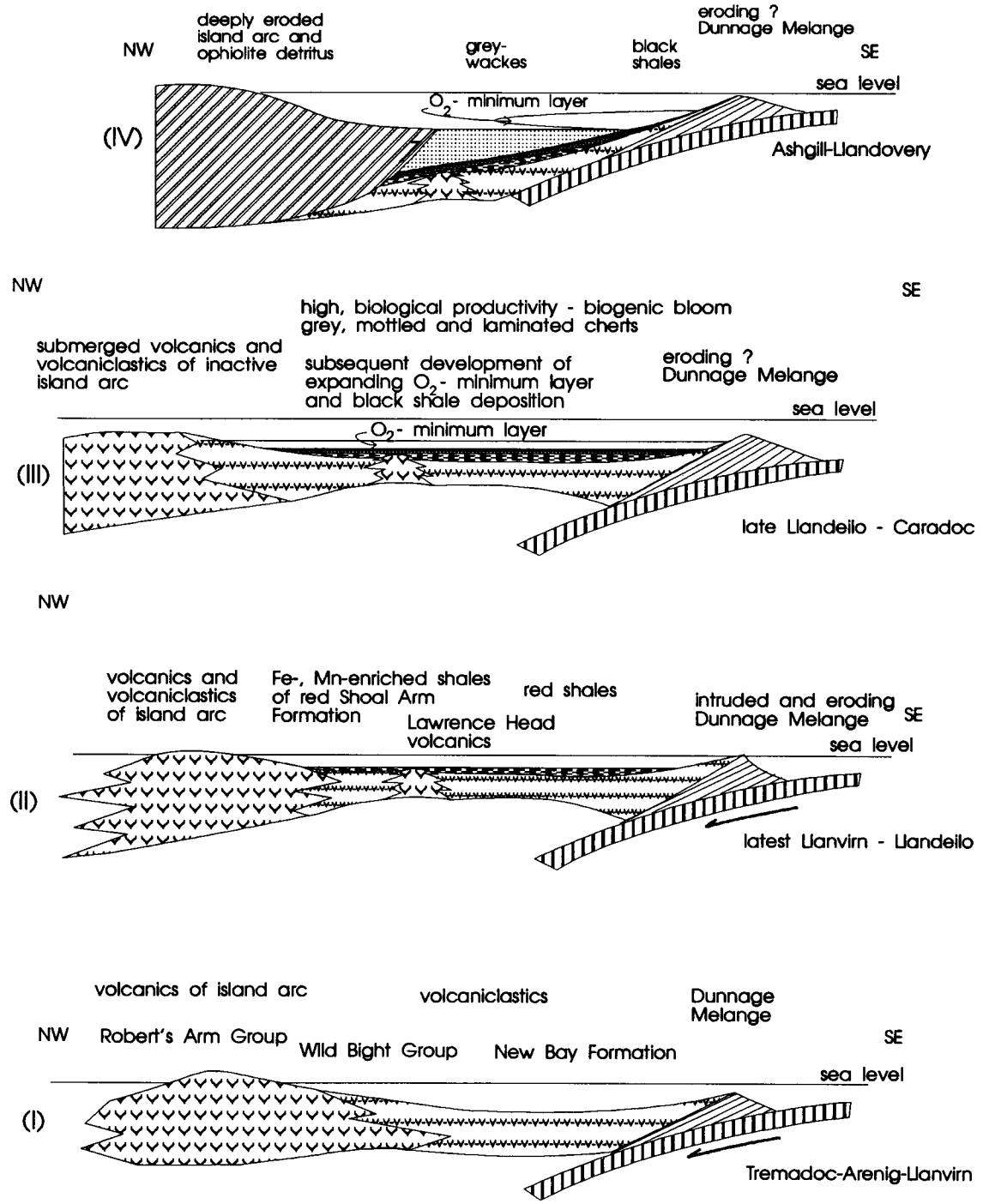

Figure 9. Tectonic model illustrating the evolution of the Shoal Arm Formation from Early Ordovician to Early Silurian. The model proposes that deposition of both the red and the grey Shoal Arm Formation units had ended everywhere by the time the black shales were deposited. The model thus implies synchronous deposition of each unit across the basin. Increasing biological productivity, seen in the deposition of the grey cherts, controls the change to increasingly anoxic conditions (black slates). A global anoxic event would be responsible for the black shale deposition.

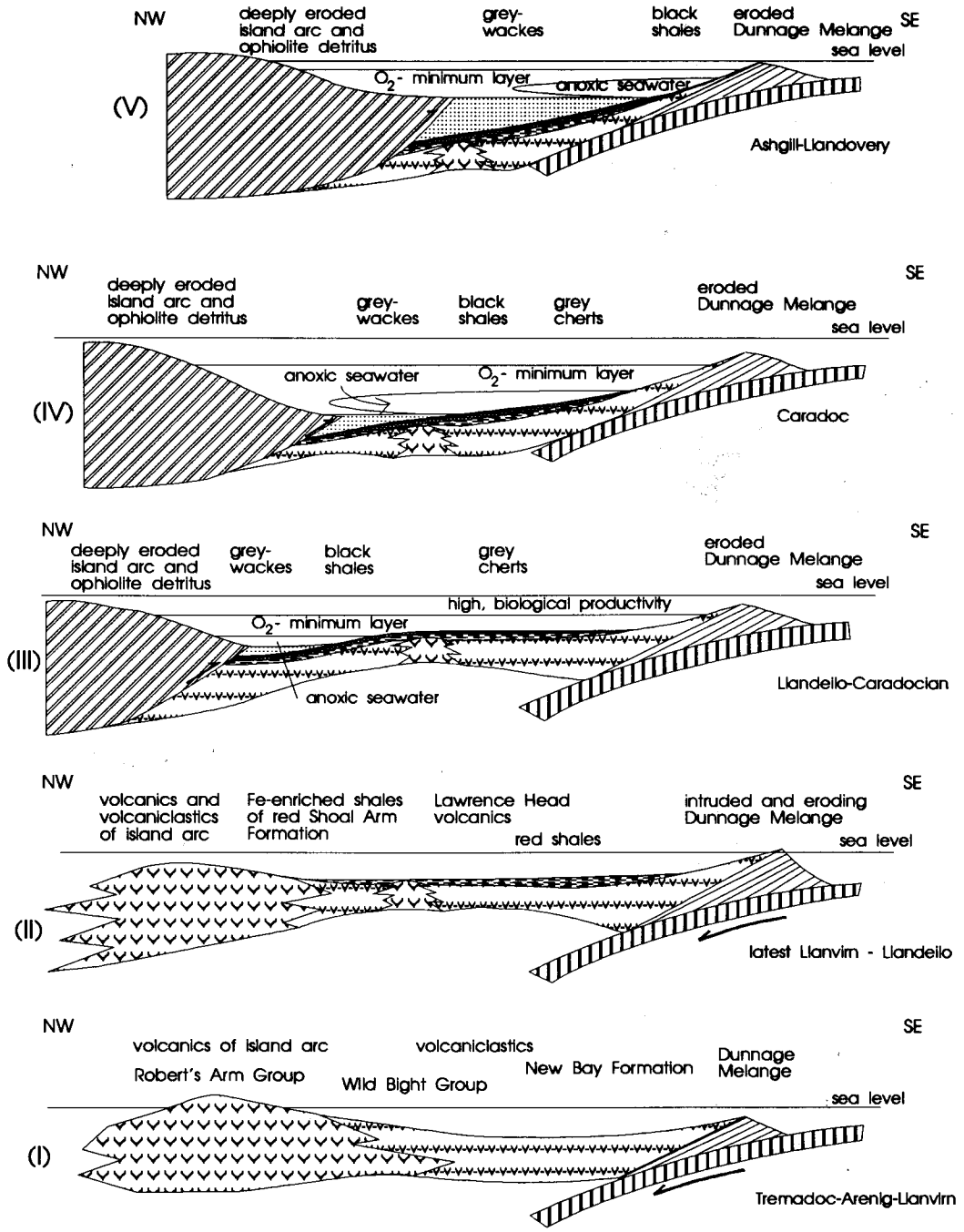

Figure 10. Alternative tectonic model illustrating the evolution of the Shoal Arm Formation from Early Ordovician to Early Silurian. In contrast to the previous model, the grey and black Shoal Arm Formation were deposited diachronously to the SE and preceded a migrating greywacke-filled trough and thrust stack. Black shale deposition occurred in an O_2-deficient, circulation-barried deep-water layer in a stratified water column in the deepest parts of the basin. As the thrust stack moved across the basin, this O_2-deficient water layer and the location of black shale deposition were transferred in the direction of thrust movement and always preceded the arrival of the greywackes from the thrust stack.

would have resulted in the enhanced deposition of organic material on the seafloor, evidenced by higher abundances of Ba and Si in the gray cherts. Accumulation of this material would have ended the mainly oxic, diagenetic conditions of the red Shoal Arm Formation. The change from red argillites to grey cherts to black slates may therefore reflect such strong biological productivity that the basin was deoxygenated by organic carbon oxidation. This scenario requires that a thermocline below the wave base prohibited O_2-renewal in the zone of high biological productivity. Due to restricted circulation and O_2-drain by organic carbon oxidation in the zone of high biological productivity, the deep water would have become increasingly depleted in O_2, which eventually resulted in anoxic conditions and black shale deposition. According to this model, the black shales may be coincident with a worldwide "Oceanic Anoxic Event" (e.g., Schlanger and Jenkyns 1976), since black shales of similar age have also been reported from other parts of the world (e.g., Leggett 1981; Hay and Cisne 1988, Bruton 1984). The effect of continuous O_2-depletion was possibly enhanced by the topography of the basin. The Dunnage Mélange to the east (figure 1), has been interpreted as an accretionary prism (Dewey et al. 1983; van der Pluijm and van Staal 1988), inactive by Caradocian times due to spreading ridge subduction (Kidd et al. 1977). This topographic high may have been a sill for influxing open-ocean, O_2-rich seawater. The deposition of grey cherts and black slates therefore took place during tectonic and volcanic quiescence, similar to that proposed for this part of the Taconic Orogen during the Caradocian (e.g., Nelson 1979; Arnott et al. 1985; Dewey et al. 1983). The deposition of the greywackes of the Gull Island Formation then marked a change of environments by the renewal of a clastic source that prograded over the basin from NW to SE (figure 9.IV).

Arnott et al. (1985) proposed that the onset of greywacke sedimentation in the Exploits zone occurred time-transgressively to the E and SE, but suggested that black shale sedimentation was synchronous and started at the base of the *Nemagraptus gracilis zone* (Arnott et al. 1985, p. 609). We believe there is insufficient fossil evidence to constrain the onset of black shale deposition synchronously or diachronously. The black shales differ from the grey cherts only in the amount of clastic material diluting the biogenic component, implying that the clastic component of the black shales is the initial clastic influx that coarsens upward into the greywackes of the flysch. Consequently, the black shales may have been deposited diachronously to the SE, similar to the overlying greywackes (Arnott et al. 1985). Since onset of black shale deposition probably reflects anaerobic/anoxic bottom-water conditions, different ages of the black slates indicate that such conditions also developed diachronously in the direction of greywacke progradation. These aspects are emphasized in model 2 and are illustrated in figure 10.III–V. The model emphasizes the subsidence effect that a thrust stack approaching from the NW would have imposed on the basin. As the thrust stack migrated to the SE, it would cause the basin to form an asymmetric trough prograding in the direction of thrust movement.

The SE-directed thrusting of a deeply eroded arc and ophiolite fragments (Nelson 1979) caused the NW part of the basin to subside first. Water circulation may have been restricted in these deepest parts of the basin so that O_2-deficient bottom-waters developed and black shales were deposited. These anoxic conditions developed diachronously prograding SE in front of the trough. The deepest parts of this trough were filled with greywackes derived from the uplifted terrane in the N and NW. Possibly, the deepest parts of the basin were ventilated again with greywacke deposition, assuming that the turbulent currents contained O_2-rich waters from shallower depths. On the SE side of the trough, the lower slope of the basin was still anaerobic, and sedimentation rates remained low. In these parts, black shale deposition continued. Farther upslope, the seafloor was still located within a dysaerobic zone characterized by high biogenic accumulation rates resulting from high biological productivity in the photic zone. Here, grey cherts accumulated. We proposed that the amount of biogenic material supplied to the basin floor during the highest biological productivity controlled the change from oxic/suboxic conditions (red argillites) to anaerobic conditions (grey cherts). Anoxic conditions were then achieved as the basin floor subsided into the euxinic, stagnant deep-water layer. Within continued basin subsidence from thrust progradation, those parts of the basin located to the SE were also subject to this transition.

Conclusions

Model 2 provides an explanation of the 10-fold Mn-enrichment (relative to PAAS) in the upper part of the red and in the grey Shoal Arm Formation (figure 7). Evidence of a possible hydrothermal contribution to the Mn abundances exists only for the lower part of the red Shoal Arm Formation. It is difficult to explain the Mn-enrichment in the

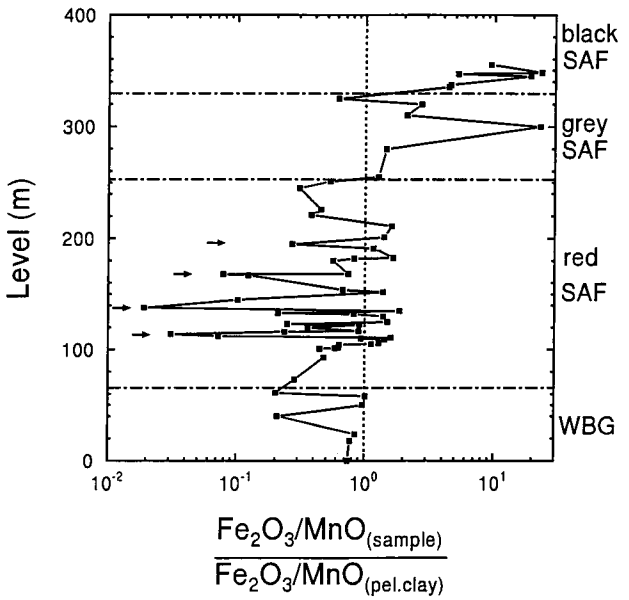

Figure 11. Stratigraphic trend of the Fe/Mn ratio to illustrate the fractionation of Mn from the less mobile element Fe. Only in the black slates of the Shoal Arm Formation does the Fe/Mn ratio change substantially to higher ratios, indicating preferred mobilization of Mn. The diagram suggests that deoxygenation of the basin was not strong enough to mobilize substantial amounts of Fe from the sediment. Although episodic, dysaerobic conditions may already have existed in the grey cherts, for the red Shoal Arm Formation oxygen conditions in the basin appear to have been high enough to inhibit Mn recycling from the sediment back to the seawater. Substantial variation of the Fe/Mn ratio in the lower Shoal Arm Formation is most likely due to localized diagenetic mobility of Mn and the formation of the highly Mn-enriched Mn,Ca-carbonate bands (indicated by arrows).

upper part of the Shoal Arm Formation by hydrothermal enrichment—in particular since the presumed volcanic source, the Lawrence Head volcanics, may already have been eroded by that time. In model 2, O_2-deficient water masses would have existed in one part of the basin at the same time as oxic conditions prevailed in another part (figure 10). Conceivably, higher concentrations of Mn^{2+} existed in this suboxic and anoxic water layer because Mn would have been recycled in reduced form from the sediment back to the seawater in the already anoxic/suboxic parts of the basin (Jenkyns et al. 1991; Pratt et al. 1991; Force and Cannon 1988). This Mn^{2+} could subsequently have been transported by bottom currents to the more oxygenated parts of the basin, where it would have been reoxidized and precipitated (Jenkyns et al. 1991; Pratt et al. 1991; Force and Cannon 1988). The increase in the Fe/Mn ratio in the black slates (figure 11), and the relatively stronger Mn depletion compared to Fe in the black slates (figures 6 and 7) illustrate that the deoxygenation of the basin apparently resulted in effective fractionation of Mn from the less mobile element Fe and suggest that redox conditions during black shale deposition were favorable to dissolve Mn from the sediment without substantial dissolution of Fe. The diachronous development of O_2-deficient water conditions would thus have permitted transport of Mn within the basin without the need of an external source (e.g., hydrothermal material, or, very unlikely in this depositional environment, continent-derived lateritic material). Most important, this process may explain Mn-enrichment in ancient deep-marine foreland basin sediments that show no association with volcanism. For the reasons discussed above, we prefer the diachronous model, since (a) this model provides a conceivable source for the Mn-enrichment observed in the grey cherts and the upper red Shoal Arm Formation, and (b) the diachronous deposition of the Shoal Arm Formation, at least from the black shales on, is more consistent with the general geology and the tectonics of the Exploits Zone. At present, it is not possible to quantify the amount of Mn, and possibly Fe, that was recycled, since this process is dependent on a variety of parameters (e.g., the degree of deoxygenation of the basin, the amount of reduced material released to the seawater and actually transported away—in contrast to local recycling, and the process of refixation). Many of these problems require further research in modern sediments before an application to ancient sediments can be made.

ACKNOWLEDGMENTS

We thank Coeditor Robert C. Newton and three anonymous reviewers for helpful comments on this manuscript. Financial support for this study comes from grants by the SUNY Benevolent Fund and Sigma XI awarded to V.B.

REFERENCES CITED

Argast, S., and Donnelly, T. W., 1987, The chemical discrimination of clastic sedimentary components: Jour. Sed. Petrol., v. 57, p. 813–823.

Arnott, R. J.; McKerrow, W. S.; and Cocks, L. R. M., 1985, The tectonics and depositional history of the Ordovician and Silurian rocks of Notre Dame Bay,

Newfoundland: Can. Jour. Earth Sci., v. 22, p. 607–618.

Basaltic Volcanism Study Project, 1981, Basaltic volcanism on the terrestrial planets: New York, Pergamon Press, 1286 p.

Berner, R. A., 1984, Sedimentary pyrite formation: an update: Geochim. Cosmochim. Acta, v. 48, p. 605–615.

Bischoff, R. J., and Rosenbauer, J. L., 1983, Uptake and transport of heavy metals by heated seawater: a summary of the experimental results, *in* Rona, P. A.; Boström, K.; et al. eds., Hydrothermal Processes at Seafloor Spreading Centers: New York, Plenum, p. 177–196.

Brongersma-Sanders, M., 1983. Unconsolidated phosphorites, high barium, and diatom abundances in some Namibian shelf sediments, *in* Thiede J., and Suess, E., eds., Coastal Upwelling, Its Sediment Record; Part A: Response of the Sedimentary Regime to Present Coastal Upwelling: New York, Plenum, p. 421–437.

Bruton, D. L., 1984, Aspects of the Ordovician system: paleontological contributions from the University of Oslo No. 295, Oslo, Universitaetsforlaget, 228 p.

Calvert, S. E., 1974, Deposition and diagenesis of silica in marine sediments, *in* Hsü, K. J., and Jenkyns, H. C., eds., Pelagic Sediments: On Land and under the Sea (Spec. Pub. Int. Assoc. Sediment. 1): Blackwell, Oxford, p. 273–299.

Chester, R., and Aston, S. R., 1976, Geochemistry of deep-sea sediments, *in* Riley, J. P., and Chester, R., Chemical Oceanography, Vol. 6: New York, Academic Press, p. 281–390.

Dean, P. L., 1978, The volcanic stratigraphy and metallogeny of Notre Dame Bay, Newfoundland: Memorial Univ. Newfoundland Geol. Rep. 7, 204 p.

Dean, W. E.; Arthur, M. A.; and Stow, D. A. V., 1984, Origin and geochemistry of Cretaceous black shales and multicolored claystones, with emphasis on Deep Sea Drilling Project site 530, southern Angola Basin, *in* Hay, W. W.; Sibuet, J. C., et al., eds., Initial Reports of the Deep Sea Drilling Project, 75: Washington D.C., U.S. Gov. Printing Office, p. 819–843.

Dewey, J. F.; Kennedy, M. J.; and Kidd, W. S. F., 1983, A geotraverse through the Appalachians of northern Newfoundland, *in* Profiles of Orogenic Belts (Geodynamic Series 10): Am. Geophysical Union, p. 205–241.

Dymond, J., 1981, Geochemistry of Nazca Plate surface sediments: an evaluation of hydrothermal, biogenic, and hydrogenous sources, *in* Kulm, L. D.; Dymond, J.; et al., eds., Nazca plate: crustal formation and Andean convergence: Geol. Soc. America Mem. 154, p. 133–173.

Förstner, U., 1982*a*, Chemical forms of metal enrichment in recent sediments, *in* Amstutz, G., Ore Genesis: Heidelberg, Springer-Verlag, p. 191–99.

Force, E. R., and Cannon, W. F., 1988, Depositional model for shallow marine manganese deposits around black shale basins: Econ. Geol., v. 83, p. 93–117.

Frakes, L. A., and Bolton, B. R., 1984, Origin of manganese giants: sea level change and anoxic-oxic history: Geology, v. 12, p. 83–86.

Glasby, G. P., 1991, Mineralogy, geochemistry, and origin of Pacific red clays: a review: New Zealand Jour. Geol. Geophys., v. 34, p. 167–176.

Hay, B. J., and Cisne, J. L., 1988, Deposition in the oxygen-deficient Taconic foreland basin, Late Ordovician, *in* Keith, B. D., ed., The Trenton Group (upper Ordovician series) of North-America: AAPG Studies in Geology 29, p. 113–134.

Heath, G. R., and Dymond, J., 1977, Genesis and transformation of metalliferous sediments from the East Pacific Rise, Bauer Deep, and Central basin, northwest Nazca plate: Geol. Soc. America Bull., v. 88, p. 723–733.

———, and ———, 1981, Metalliferous sediment deposition in time and space: East Pacific Rise and Bauer Basin, northern Nazca Plate, *in* Kulm, L. D.; Dymond, J.; et al., eds., Nazca plate: crustal formation and Andean convergence: Geol. Soc. America Mem. 154, p. 175–198.

Heggie, D.; Klinkhammer, G. P.; and Cullen, D., 1987, Manganese and copper fluxes from continental margin sediments: Geochim. Cosmochim. Acta, v. 51, p. 1059–1070.

Helwig, J., 1967, Stratigraphy and structural history of the New Bay area, north central Newfoundland: Unpub. Ph.D. dissertation, Columbia University, New York, 212 p.

Hudson, A.; Bender, M. L.; and Graham, D. W., 1986, Iron enrichments in hydrothermal plumes over the East Pacific Rise: Earth Planet. Sci. Lett., v. 79, p. 250–254.

Jacobi, R. D., and Wasowski, J. J., 1985, Geochemistry and plate-tectonic significance of the volcanic rocks of the Summerford Group, north-central Newfoundland: Geology, v. 13, p. 126–130.

Jarvis, I., and Higgs, N., 1987, Trace element mobility during early diagenesis in distal turbidites: Late Quaternary of Madeira Abyssal Plain, North Atlantic, *in* Weaver, P. P. E., and Thomson, J., eds., Geology and Geochemistry of Abyssal Plains: Geol. Soc. (London) Spec. Pub. 31, p. 179–214.

Jenkyns, H. C., 1980, Cretaceous anoxic events: from continents to oceans: Jour. Geol. Soc. London, v. 137, p. 171–188.

———; Geczy, B.; and Marshall, J. D., 1991, Jurassic manganese carbonates of central Europe and the early Toarcian anoxic event: Jour. Geology, v. 99, p. 137–149.

Kusky, T. M., 1985, Geology of the Frozen Ocean Lake–New Bay Pond area, north-central Newfoundland: Unpub. M.Sc. thesis, SUNY Albany, 214 p.

Leggett, J. K., 1980, British lower Paleozoic shales and their paleo-oceanographic significance: Jour. Geol. Soc. London, v. 137, p. 139–156.

———, 1982, Geochemistry of Cocos plate pelagic hemipelagic sediments in hole 487, Deep Sea Drilling Project 66, *in* Watkins J. S.; Moore, J. C.; et al., Initial Reports of the Deep Sea Drilling Project, 66: Washington, D.C., U.S. Gov. Printing Office, p. 683–686.

———; McKerrow, W. S.; Cocks, L. R. M.; and Rickards, R. B., 1981, Periodicity in the Paleozoic realm: Jour. Geol. Soc. London, v. 138, p. 167–176.

Leinen, M., 1987, The origin of paleochemical signatures in North Pacific pelagic clays: partitioning experiments: Geochim. Cosmochim. Acta, v. 51, p. 305–319.

Kidd, W. S. F.; Dewey, J. F.; and Nelson, K. D., 1977. Medial Ordovician ridge subduction in central Newfoundland: Geol. Soc. America Abs. with Prog., v. 9, p. 283–284.

Martin, J. H., and Knauer, G. A., 1973, The elemental composition of plankton: Geochim. Cosmochim. Acta, v. 37, p. 1639–1654.

McKerrow, W. S., 1979, Ordovician and Silurian changes in sea level: Jour. Geol. Soc. London, v. 136, p. 137–145.

———; Leggett, J. K.; and Eales, M. H., 1977, Imbricate thrust model of the Southern Uplands of Scotland: Nature, v. 267, p. 237–239.

McMurty, G. M.; Veeh, H. H.; and Moser, C., 1981, Sediment accumulation rate patterns on the northwest Nazca Plate, *in* Kulm, L. D.; Dymond, J.; et al., eds., Nazca plate: crustal Formation and Andean convergence: Geol. Soc. America Mem. 154, p. 211–250.

Minoura, K.; Nakaya, S.; and Takemura, A., 1991, Origin of manganese carbonates in Jurassic red shale: Sedimentology, v. 38, p. 137–152.

Nelson, K. D., 1979, Geology of the Badger Bay–Seal Bay area, north-central Newfoundland: Unpub. Ph.D. dissertation, SUNY Albany, 184 p.

———, 1981, Mélange development in the Boones Point Complex, north-central Newfoundland: Can. Jour. Earth Sci., v. 18, p. 433–442.

———, and Casey, J. D., 1979, Ophiolite detritus in the upper Ordovician flysch of Notre Dame Bay and its bearing on the tectonic evolution of western Newfoundland: Geology, v. 7, p. 27–31.

Pedersen, T. F., and Price, N. B., 1982, The geochemistry of manganese carbonate in Panama basin sediments: Geochim. Cosmochim. Acta, v. 46, p. 59–68.

Pickering, K. T.; Bassett, G.; and Siveter, D. J., 1988, Late Ordovician–Early Silurian destruction of the Iapetus Ocean: Newfoundland, British Isles, and Scandinavia—a discussion: Trans. Royal Soc. (Edinburgh), v. 79, p. 361–382.

Pomerol, B., 1983, Carbon isotopes and Mn-variations in Cenomanian chalks of the Paris basin: Cretaceous Research, v. 4, p. 85–93.

Pratt, L.; Force, E. R.; and Pomerol, B., 1991, Coupled manganese and carbon isotope events in marine carbonates at the Cenomanian-Turonian boundary: Jour. Sed. Petrol., v. 61, p. 370–383.

Rast, N., and Stringer, P., 1980, A geotraverse across a deformed Ordovician ophiolite and its Silurian cover, northern New Brunswick: Tectonophysics, v. 69, p. 221–245.

Rowley, D. B., and Kidd, W. S. F., 1981, Stratigraphic relationships and detrital composition of the medial Ordovician flysch of western New England: implications for the tectonic evolution of the Taconic orogeny: Jour. Geology, v. 89, p. 199–218.

Sawlan, J. J., and Murray, J. W., 1983, Trace metal mobilization in the interstitial waters of red clay and hemipelagic marine sediments: Earth Planet. Sci. Lett., v. 64, p. 213–230.

Scholle, P. A., and Arthur, M. A., 1980, Carbon isotope fluctuations in Cretaceous pelagic limestones: potential stratigraphic and exploration tool: AAPG Bull., v. 64, 67–87.

Schlanger, S. O., and Jenkyns, H. C., 1976, Cretaceous anoxic events: causes and consequences: Geologie en Mijnbouw, v. 55, p. 179–184.

Seyfried, W. E., and Janecky, D. R., 1985, Heavy metal and sulfur transport during subcritical and supercritical hydrothermal alteration of basalt: influence of fluid pressure and basalt composition and crystallinity: Geochim. Cosmochim. Acta, v. 49, p. 2545–2560.

Stoffers, P.; Schmitz, W.; et al., 1985, Mineralogy and geochemistry of sediments in the Southwestern Pacific Basin: Tahiti–East Pacific Rise—New Zealand: New Zealand Jour. Geol. Geophysics, v. 28, p. 235–259.

Swinden, H. S.; Jenner, G. A.; et al., 1990, Petrogenesis and paleotectonic history of the Wild Bight Group, an Ordovician island arc in central Newfoundland: Contrib. Mineral. Petrol., v. 105, p. 219–241.

Taylor, S. R., and McLennan, S. M., 1985, The Continental Crust: Its Composition and Evolution, Oxford, Blackwell, 312 p.

Thickpenny, A., and Leggett, J. K., 1987, Stratigraphic distribution and palaeooceanographic significance of European early Paleozoic organic-rich sediments, *in* Brooks, J., and Fleet, A. J., eds., Marine Petroleum source rocks: Geol. Soc. (London) Spec. Pub. 26, p. 231–247.

Thomson, J.; Higgs, N. C.; et al., 1986, The behavior of manganese in Atlantic carbonate sediments: Geochim. Cosmochim. Acta, v. 50, p. 1807–1818.

Van der Pluijm, B. A., and van Staal, C. R., 1988, Characteristics and evolution of the central mobile belt, Canadian Appalachians: Jour. Geology, v. 96, p. 535–547.

Vine, J. D., and Tourtelot, E. B., 1970, Geochemistry of black shale deposits—a summary report: Econ. Geol., v. 65, p. 253–272.

Williams, S. H., and Rickards, R. B., 1984, Paleoecology of graptolitic black shales, *in* Bruton, D. L., ed., Aspects of the Ordovician System: Paleontological contributions from the University of Oslo, No. 295, Oslo, Universitaetsforlaget, p. 159–166.